

Heat resistance of carbon nanoionions by molecular dynamics simulation

Xianqiao Wang* and James D. Lee

*Department of Mechanical and Aerospace Engineering, The George Washington University,
Washington, DC 20052, USA*

(Received June 5, 2011, Revised October 23, 2011, Accepted October 24, 2011)

Abstract. Understanding the structural stability of carbon nanostructure under heat treatment is critical for tailoring the thermal properties of carbon-based material at small length scales. We investigate the heat resistance of the single carbon nanoball (C_{60}) and carbon nanoionions ($C_{20}@\mathcal{C}_{80}$, $C_{20}@C_{80}@C_{180}$, $C_{20}@C_{80}@C_{180}C_{320}$) by performing molecular dynamics simulations. An empirical many-body potential function, Tersoff potential, for carbon is employed to calculate the interaction force among carbon atoms. Simulation results shows that carbon nanoionions are less resistive against heat treatment than single carbon nanoballs. Single carbon nanoballs such C_{60} can resist heat treatment up to 5600 K, however, carbon nanoionions break down after 5100 K. This intriguing result offers insights into understanding the thermal-mechanical coupling phenomena of nanodevices and the complex process of fullerenes' formation.

Keywords: molecular dynamics; carbon nanoballs; carbon nanoionions; heat resistance; tersoff potential.

1. Introduction

Understanding and controlling the thermomechanical coupling behaviors of nanostructures, such as carbon nanotubes, buckyballs, and graphene, is a key issue in nanotechnology. Numerous studies, both experimental (Sazonova *et al.* 2004, Dong *et al.* 2006) and theoretical (Kral and Sadeghpour 2002, Fleishman *et al.* 2007, Xu *et al.* 2007), have been devoted to nanoelectromechanical systems at molecular level. Ever since it was discovered almost two decades ago (Kroto *et al.* 1985), C_{60} has attracted enormous attentions owing to novel structural, chemical and mechanical properties. The unique structural properties of C_{60} gives rise to its peculiar applications in biological systems, offering the promise to be a excellent candidate for drug delivery, biomedical imaging, and templates for designing pharmaceutical agents such as HIV inhibitors (Cagle *et al.* 1999, Wilson *et al.* 1999, Noon *et al.* 2002). Meanwhile, the superior mechanical properties of C_{60} make it ideally suitable for nanoelectromechanical application, for example the fabrication of nanovalves and nanoscillators (Neto and Oliveira 2010, Chen *et al.* 2011). In additional to its mechanical properties, the electrical properties of C_{60} (Chen *et al.* 1991, Hebard *et al.* 1991, Rosseinsky *et al.* 1991) have been demonstrated to be of fundamental and practical importance since it has a superior thermal

* Corresponding author, Ph.D., E-mail: xqwang@gwu.edu

conductivity like carbon nanotubes (Kim *et al.* 2001, Pop *et al.* 2006). The number of experimental works devoted to the study of C is so large that has required several review articles (Eleanor and Frank 2000, Lifshitz 2000). These effects have led to significant theoretical advances in order to understand its structure and high stability (Scuseria 1996). However, there is very little research work focusing on the thermal properties of carbon nanoions such as $C_{20}@\text{C}_{80}$, $C_{20}@\text{C}_{80}@\text{C}_{180}$, $C_{20}@\text{C}_{80}@\text{C}_{180}\text{C}_{320}$. Therefore, it is necessary to investigate their thermal stability through molecular dynamics simulations.

In this paper, we present a molecular dynamics simulation study of the heat resistance of the single carbon nanoball (C_{60}) and carbon nanoions ($\text{C}_{20}@\text{C}_{80}$, $\text{C}_{20}@\text{C}_{80}@\text{C}_{180}$, $\text{C}_{20}@\text{C}_{80}@\text{C}_{180}\text{C}_{320}$). Our paper is arranged as follows. In section 2, the computational model and methods used in the simulation is introduced. The results of our simulations are presented in section 3. Finally, conclusions and directions for future studies are discussed in section 4.

2. Computational model and method

The nano system consisting of carbon nanoballs or carbon nanoions is performed by molecular dynamics simulation, where the interatomic interactions between carbon and carbon are described using Tersoff potential (Tersoff 1989). The interatomic potential is taken to have the form

$$E = \sum_i E_i = \frac{1}{2} \sum_{i \neq j} V_{ij} \quad (1)$$

$$V_{ij} = f_c(r_{ij})[f_R(r_{ij}) + b_{ij} f_A(r_{ij})] \quad (2)$$

Here E is the total energy of the system, which is decomposed for convenience into a size energy E_i and a bond energy V_{ij} . The indices i and j run over the atoms of the system, and r_{ij} is the distance from atom to atom. b_{ij} represents a measure of the bond order, and is assumed to be a monotonically decreasing function of the coordination of atom i and j . The function f_R represents a repulsive pair potential, and f_A represents an attractive pair potential associated with bonding. The extra term f_c is merely a smooth cutoff function, to limit the range of the potential, since for many applications short-ranged functions permit a tremendous reduction in computational effort.

Here the functions f_R , f_A and f_c are simply taken as

$$f_R(r_{ij}) = A_{ij} \exp(-\lambda_{ij} r_{ij}) \quad (3)$$

$$f_A(r_{ij}) = -B_{ij} \exp(-\mu_{ij} r_{ij}) \quad (4)$$

$$f_c(r_{ij}) = \begin{cases} 1, & r_{ij} < R_{ij} \\ \frac{1}{2} + \frac{1}{2} \cos[\pi(r_{ij} - R_{ij})/(s_{ij} - R_{ij})], & R_{ij} < r_{ij} < S_{ij} \\ 0, & r_{ij} > S_{ij} \end{cases} \quad (5)$$

where

$$\begin{aligned}
 b_{ij} &= \chi_{ij}(1 + \beta_i^n \xi_{ij}^{n_i})^{-1/2n_i} \\
 \xi_{ij} &= \sum_{k \neq i,j} f_c(r_{ik}) \omega_{ik} g(\theta_{ijk}) \\
 g(\theta_{ijk}) &= 1 + c_i^2/d_i^2 - c_i^2/[d_i^2 + (h_i - \cos \theta_{ijk})^2] \\
 \omega_{ij} &= 1, \quad \chi_{ij} = 1 \\
 A_{ij} &= (A_i A_j)^{1/2}, \quad B_{ij} = (B_i B_j)^{1/2}, \quad \lambda_{ij} = (\lambda_i + \lambda_j)/2, \quad \mu_{ij} = (\mu_i + \mu_j)/2, \\
 R_{ij} &= (R_i R_j)^{1/2}, \quad S_{ij} = (S_i S_j)^{1/2}
 \end{aligned} \tag{6}$$

Here i, j and k labels the atoms of the system, θ_{ijk} is the bond angle between bond ij and ik . Single subscripted parameters, such as $A_i, B_i, S_i, R_i, \lambda_i, n_i$, and μ_i , are material constants depending on the type of atom (C , Si or Ge). The energy is modeled as a sum of pairlike interactions, where, however, the coefficient of the attractive term in the pairlike potential depends on the local environment, giving a many-body potential. The material constants of carbon are presented in detail as follows

$$\begin{aligned}
 A &= 1.3936 \times 10^6 \text{ eV}, \quad B = 3.467 \times 10^2 \text{ eV}, \quad \lambda = 3.4879 \times 10^{-1} \text{ nm}, \quad \mu = 2.2119 \times 10^{-1} \text{ nm}, \\
 \beta &= 1.5724 \times 10^7, \quad n = 7.2751 \times 10^{-1}, \quad c = 3.8049 \times 10^4, \quad d = 4.384, \quad h = -5.7058 \times 10^{-1}, \\
 R &= 1.8 \times 10^{-1} \text{ nm} \quad S = 2.1 \times 10^{-1} \text{ nm}
 \end{aligned}$$

Temperature at nano scale is a dependent statistical variable, which is derived from the velocity of a specified group of atoms. In this work, the carbon nanoballs or nanoion are considered as a group, and temperature is defined as a space-averaged variable of atoms in the whole group

$$T(t) = \frac{\sum_{i=1}^N m_i [\mathbf{v}_i(t) - \bar{\mathbf{v}}]^2}{3k_B N} \tag{7}$$

where N is the number of the group of atoms; m_i is the mass of atom i ; \mathbf{v}_i is the velocity of atom i ; $\bar{\mathbf{v}}$ is the average velocity of the group of atoms; k_B is the Boltzmann constant.

The evolution of the atoms in the system under heat treatment is ruled by the equation

$$m^i \ddot{\mathbf{x}}^i(t) = \mathbf{f}^i(t) - m^i \chi(t) [\mathbf{v}^i(t) - \bar{\mathbf{v}}] \tag{8}$$

where $\mathbf{x}^i(t)$ is the position of the i -th atom; $\mathbf{f}^i(t)$ is the interatomic force acting on the i -th atom; $\dot{\mathbf{x}}^i(t) = d\mathbf{x}^i(t)/dt$; $\ddot{\mathbf{x}}^i(t) = d^2\mathbf{x}^i(t)/dt^2$; χ is the friction coefficient modeling the microscopic action of the Nosé-Hoover thermostat to control the temperature. The dynamics of χ is governed by the equation

$$\frac{d\chi(t)}{dt} = \frac{1}{Q} \left(\sum_{j=1}^N m^j (\dot{\mathbf{x}}^j(t) - \bar{\mathbf{v}}(t))^2 - 3k_B N T_{eqb} \right) \tag{9}$$

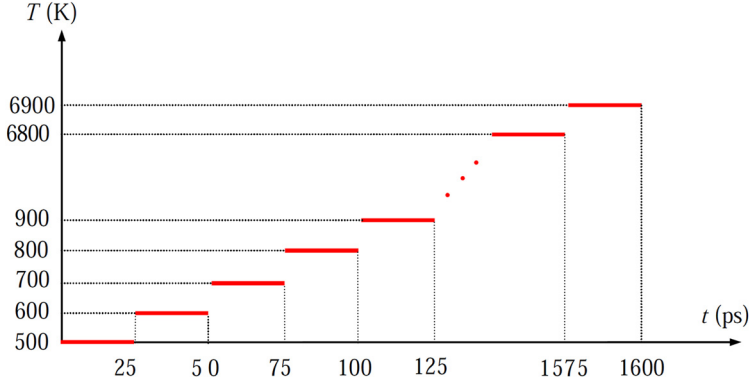


Fig. 1 Temperature profile of the system at different time

where T_{eqb} is the equilibrium or expected temperature of the group; $Q = 3Nk_B T_{eqb} \tau_T^2$ is the effective ‘mass’ of the thermostat; τ_T is a specified time constant (normally in the range [0.5, 2] ps). The action of the thermostat can be understood in the following terms. Whenever the (kinetic) temperature of the atoms in the system T is larger than T_{eqb} , $\chi(t)$ increases and eventually becomes positive. Accordingly, the friction acts as a dissipation agent which will reduce the temperature. Since the opposite occurs whenever the temperature falls below T_{eqb} , the Nosé-Hoover thermostat represented by $-m^i \chi(t) \dot{x}^i(t)$ acts as a stabilizing feedback around the prescribed temperature.

The temperature scaling by the Nosé-Hoover thermostat is taken into account at every MD step. Before starting the simulation, 50 ps Nosé-Hoover thermal bath coupling ($T = 500$ K, time step $\Delta t = 0.5$ fs) are conducted to reach a thermal equilibration of the whole system. Afterward, the temperature of the system is controlled, by Nosé-Hoover thermostat, as

$$T = 500 + 100 \times \text{Integer}\left[\frac{t}{25\text{ps}}\right] \text{ (K)} \quad t \leq 1600 \text{ ps} \quad (10)$$

where $\text{Integer}[a]$ returns the largest integer that does not exceed the range of a . The temperature profile expressed in Eq. (10) is a step function shown in Fig. 1, each step yielding a thermal equilibration with specified temperature through the Nosé-Hoover thermostat. We increase the temperature of heat bath in steps of $\Delta T = 100$ K from 500 K to the final temperature 6,900 K, and let the nanoionions equilibrate for 25 ps at each new temperature.

3. Results

In order to identify the characteristic of the individual phases, the structural evolution at various temperature for the carbon nanoball C_{60} , and carbon nanoionions $C_{20}@C_{80}$, $C_{20}@C_{80}@C_{180}$, and $C_{20}@C_{80}@C_{180}C_{320}$ are shown in Figs. 2-5, respectively. It is noticed that, C_{60} can maintain its stable cage structure up to 5600 K, and its bond begins to break at about 5700 K, which is in good agreement with the value simulated by Erkoc (2002). On the other hand, it is also observed that carbon nanoionions $C_{20}@C_{80}$, $C_{20}@C_{80}@C_{180}$, and $C_{20}@C_{80}@C_{180}C_{320}$ can keep their stable structure up to 5100 K, 4800 K, and 4600 K, respectively; while their bonds starts to break at around 5200 K,

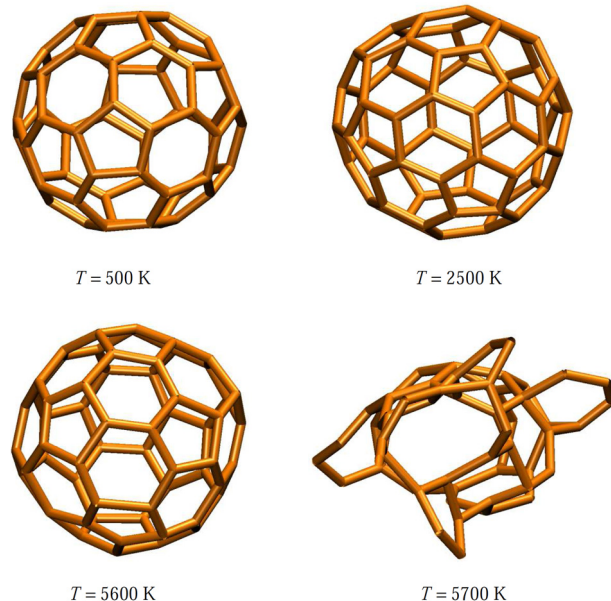


Fig. 2 Structural evolutions of carbon nanoball C_{60} over various temperatures

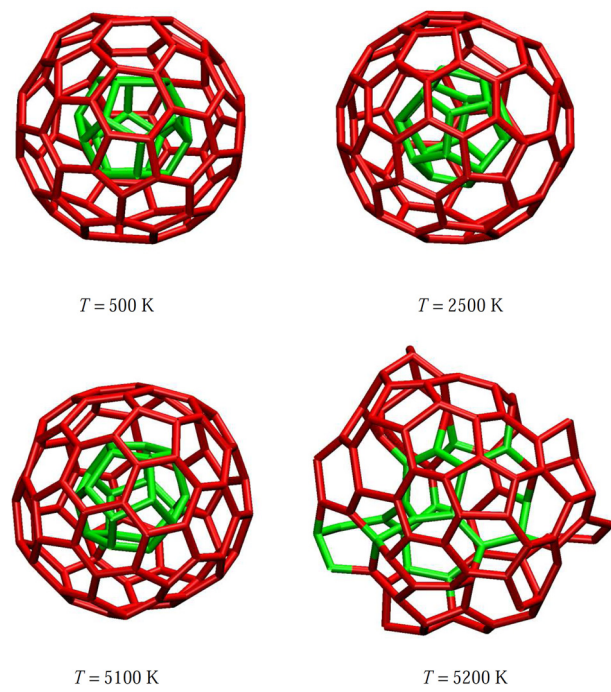


Fig. 3 Structural evolutions of carbon nanoion $C_{20}@\mathcal{C}_{80}$ over various temperatures

4900 K, and 4700 K, respectively. It is noteworthy to mention that the more layers the nanoion has, the less heat resistance the nanoion can undertake. The result of the present simulations

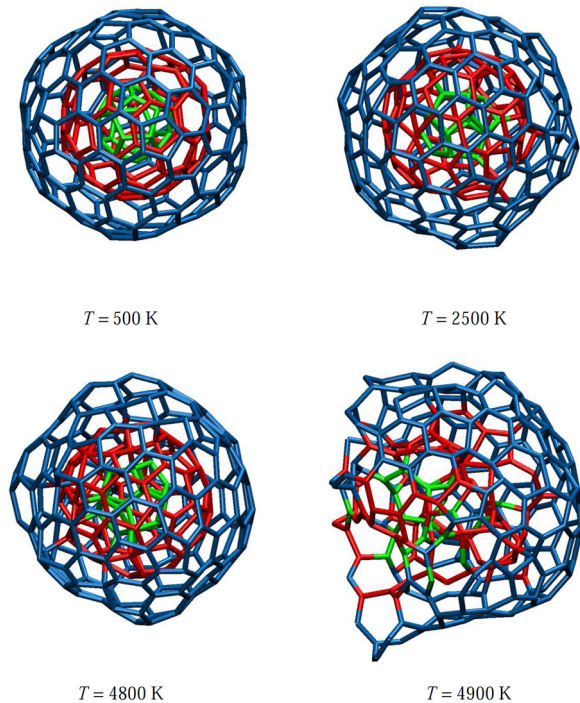


Fig. 4 Structural evolutions of carbon nanoion $C_{20} @ C_{80} @ C_{180}$ over various temperatures

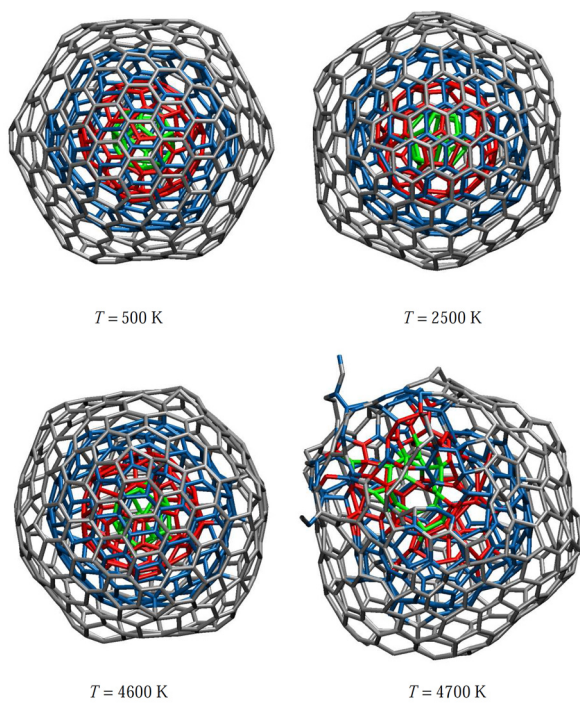


Fig. 5 Structural evolutions of carbon nanoion $C_{20} @ C_{80} @ C_{180} @ C_{320}$ over various temperatures

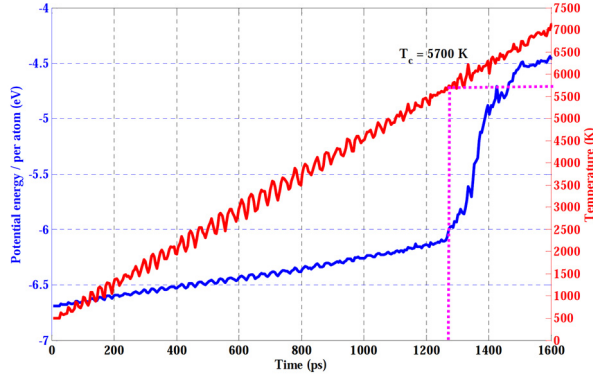


Fig. 6 Temperature and potential energy per carbon atom with respect to time for carbon nanoball C_{60}

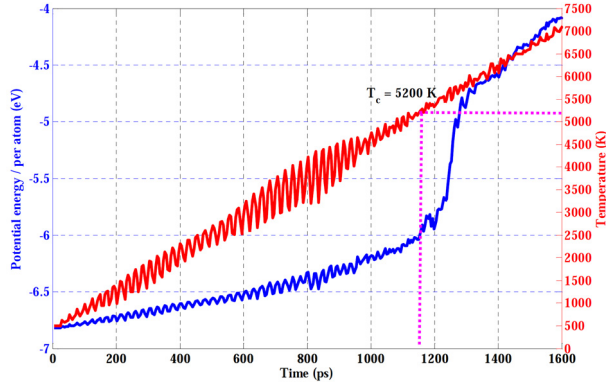


Fig. 7 Temperature and potential energy per carbon atom with respect to time for carbon nanoion $C_{20}@\mathcal{C}_{80}$

shed lights on the argument that onion-type structures of carbon nanoballs are not as resistive as the single-layered carbon nanoball against heat treatment. To get a better understanding of the structural transformations in nanoball and nanoion, we investigate the evolution of the potential energy per atom for all structures. Figs. 6-9 depict the temperature (red line) and potential energy per carbon atom (blue line) with respect to time for carbon nanoball C_{60} , carbon nanoion $C_{20}@\mathcal{C}_{80}$, $C_{20}@\mathcal{C}_{80}@C_{180}$, and $C_{20}@\mathcal{C}_{80}@C_{180}C_{320}$, respectively. It is noticed that from Figs. 6-9, as time goes, the temperature of the system (C_{60} , $C_{20}@\mathcal{C}_{80}$, $C_{20}@\mathcal{C}_{80}@C_{180}$, $C_{20}@\mathcal{C}_{80}@C_{180}C_{320}$) and the potential energy per atom increase accordingly. As expected, with the increase of temperature, the potential energy per atom first goes up steadily and then increase significantly after a critical temperature T_c . This pronounced change in potential energy per atom is correlated to the bond break of the system. Because of the similarity of the potential energy plot and the temperature profile plot for the different nanoballs or nanoions, we concentrate on the C_{60} molecule. Below 5700 K, the potential energy per atom increases linearly with temperature, indicating that there is no phase change taking place below this temperature within the time interval considered. The phase, the C_{60} molecule being intact below 5600 K, is coined as solid phase. However, when the temperature is higher than 5600 K, the energy starts to deviate from the linear behavior and grows rapidly as the temperature is increased further. Consistently, we observe that carbon-carbon bonds start to break and a dramatic

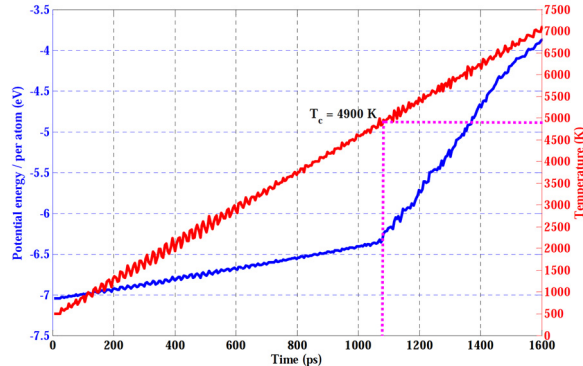


Fig. 8 Temperature and potential energy per carbon atom with respect to time for carbon nanoionions $C_{20} @ C_{80} @ C_{180}$

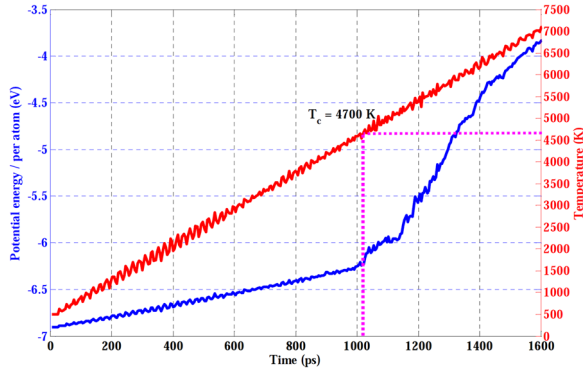


Fig. 9 Temperature and potential energy per carbon atom with respect to time for carbon nanoionions $C_{20} @ C_{80} @ C_{180} @ C_{320}$

transition from the solid phase to the pretzel phase, consisting of interconnected carbon rings shown in Fig. 2. As time goes, we can expect that the fragmentation of all fullerenes will be observed. The temperature scale relevant to structure transition in the C_{60} molecule can be linked to well established thermodynamic data for graphite (Weast 1988). We notice that the calculated disintegration temperature $T \approx 5600$ K lies close to the observed boiling point of graphite, $T \approx 5100$ K. We also find the potential energy per atom to provide a better signature of the bond break process than topological quantities such as coordination numbers which depend on the definition of cutoff distances. Thermal energy controlled by Nosé-Hoover thermostat play a vital role in the stability of the structure, which yields to the elongation and break of the bonds of nanoballs. This offers a reasonable insight into the heat resistance of carbon nanoballs or nanoionions and also sheds new light on the formation process of fullerenes from the gas phase.

4. Conclusions

This work unveils a way to study the heat resistance of carbon nanoballs or nanoionions, shedding some light into the formation mechanism and the development of efficient production method of nanoballs or nanoionions. We find that the critical stable temperature of a nanoionion depends on the

layers it has, leading to an intriguing scenario that the more layers a nanoion has the less heat resistance it endures. Moreover, the results reported in this paper feature potential for several nanotechnology applications assisted by thermal fluctuation, including the use of nanotubes as nanopipettes, and targeted drug delivery devices. However, experimental control and detection of the dynamical process of heat resistance of nanoscale systems still remain challenges.

References

- Cagle, D.W., Kennel, S.J., Mirzadeh, S., Alford, J.M. and Wilson, L.J. (1999), "In vivo studies of fullerene-based materials using endohedral metallofullerene radiotracers", *Proceedings of the National Academy of Sciences of the United States of America*, **96**(9), 5182-5187.
- Chen, C.C., Kelty, S.P., et al. (1991), "(RbxK1-x)3C60 superconductors: formation of a continuous series of solid solutions", *Science*, **253**(5022), 886-888.
- Chen, H.Y., Liu, Z.F., Gong, X.G. and Sun, D.Y. (2011), "Design of a one-way nanovalve based on carbon nanotube junction and C-60", *Microfluid. Nanofluid.*, **10**(4), 927-933.
- Dong, L., Nelson, B.J., Fukuda, T. and Arai, F. (2006), "Towards nanotube linear servomotors", *IEEE T. Autom. Sci. Eng.*, **3**(3), 228-235.
- Eleanor, E.B.C. and Frank, R. (2000), "Fullerene reactions", *Rep. Prog. Phys.*, **63**(7), 1061.
- Erkoc, S. (2002), "Stability of carbon nanoion C-20@C-60@C-240: molecular dynamics simulations", *Nano Lett.*, **2**(3), 215-217.
- Fleishman, D., Klafter, J., Porto, M. and Urbakh, M. (2007), "Mesoscale engines by nonlinear friction", *Nano Lett.*, **7**(3), 837-842.
- Hebard, A.F., Rosseinsky, M.J., Haddon, R.C., Murphy, D.W., Glarum, S.H., Palstra, T.T.M., Ramirez, A.P. and Kortan, A.R. (1991), "Superconductivity at 18 K in potassium-doped C60", *Nature*, **350**(6319), 600-601.
- Kim, P., Shi, L., Majumdar, A. and McEuen, P.L. (2001), "Thermal transport measurements of individual multiwalled nanotubes", *Phys. Rev. Lett.*, **87**(21), 215502.
- Kral, P. and Sadeghpour, H.R. (2002). "Laser spinning of nanotubes: a path to fast-rotating microdevices", *Phys. Rev. B*, **65**(16), 161401.
- Kroto, H.W., Heath, J.R., O'Brien, S.C., Curl, R.F. and Smalley, R.E. (1985), "C60: buckminsterfullerene", *Nature*, **318**(6042), 162-163.
- Lifshitz, C. (2000), "Carbon clusters", *Int. J. Mass Spectrom.*, **200**(1-3), 423-442.
- Neto, A.M.J.C. and Oliveira, C.X. (2010), "Nanoscillator and gun under temperature effect", *J. Nanosci. Nanotechnol.*, **10**(9), 5755-5758.
- Noon, W.H., Kong, Y.F. and Ma, J. (2002), "Molecular dynamics analysis of a buckyball-antibody complex", *Proceedings of the National Academy of Sciences of the United States of America*, **99**, 6466-6470.
- Pop, E., Mann, D., Wang, Q., Goodson, K. and Dai, H. (2006), "Thermal conductance of an individual single-wall carbon nanotube above room temperature", *Nano Lett.*, **6**(1), 96-100.
- Rosseinsky, M.J., Ramirez, A.P., Glarum, S.H., Murphy, D.W., Haddon, R.C., Hebard, A.F., Palstra, T.T.M., Kortan, A.R., Zahurak, S.M. and Makhija, A.V. (1991), "Superconductivity at 28 K in Rb_xC_60", *Phys. Rev. Lett.*, **66**(21), 2830.
- Sazonova, V., Yaish, Y., Ustunel, H., Roundy, D., Arias, T.A. and McEuen, P.L. (2004), "A tunable carbon nanotube electromechanical oscillator", *Nature*, **431**(7006), 284-287.
- Scuseria, G.E. (1996), "Ab initio calculations of fullerenes", *Science*, **271**(5251), 942-945.
- Tersoff, J. (1989), "Modeling solid-state chemistry: interatomic potentials for multicomponent systems", *Phys. Rev. B*, **39**(8), 5566-5568.
- Weast, R.C. (1988), *CRC handbook of chemistry and physics*, Boca Raton, FL, CRC Press.
- Wilson, L.J., Cagle, D.W., Thrash, T.P., Kennel, S.J., Mirzadeh, S., Alford, J.M. and Ehrhardt, G.J. (1999), "Metallofullerene drug design", *Coordin. Chem. Rev.*, **190-192**, 199-207.
- Xu, Z.P., Zheng, Q.S. and Chen, G. (2007), "Thermally driven large-amplitude fluctuations in carbon-nanotube-based devices: molecular dynamics simulations", *Phys. Rev. B*, **75**(19), 195445.